

## Cell-on-Hydrogel Platform Made of Agar and Alginate for Rapid, Low-cost, Multidimensional Test of Antimicrobial Susceptibility

Han Sun<sup>a</sup>, Zhengzhi Liu<sup>a</sup>, Chong Hu<sup>a</sup> and Kangning Ren<sup>\*abc</sup>

Received 00th January 20xx,  
Accepted 00th January 20xx

DOI: 10.1039/x0xx00000x

[www.rsc.org/](http://www.rsc.org/)

Antimicrobial resistance (AMR) is a rapidly increasing threat to the effective treatment of infectious diseases worldwide. Two major remedies include: (1) using narrow-spectrum antibiotics based on rapid diagnosis; (2) developing new antibiotics. A key part of both remedies is antimicrobial susceptibility test (AST). However, current standard ASTs that monitor colony formation are costly and time-consuming; new strategies proposed are not yet practical to be implemented. Herein, we report a strategy to fabricate whole-hydrogel microfluidic chips using alginate-doped agar. This agar-based microfabrication makes it possible to prepare inexpensive hydrogel devices, and allows seamless link between microfluidics and conventional agar-based cell culture. Different from common microfluidic systems, in our system the cells are cultured on top of the device, similar to normal agar plate culture; on the other hand, the microfluidic channels inside the hydrogel allow precise generation of linear gradient of drugs, giving better performance than conventional disk diffusion method. Cells in this system are not exposed to any shear flow, allowing reliable tracking of individual cells and AST result to be obtained within 2-3 hours. Furthermore, our system could test the synergistic effect of drugs through two-dimensional gradient generation. Finally, the platform could be directly implemented to new drug discovery and other applications where a fast, cost-efficient method for studying the response of microorganisms upon drug administration is sought for.

### Introduction

The development of antimicrobial resistance (AMR) is a natural phenomenon in microorganisms, and is accelerated by misuse of antibiotics.<sup>1-3</sup> AMR makes the treatment of infections difficult, costly, or even impossible. World Health Organization (WHO) warned that AMR is "a problem so serious that it threatens the achievements of modern medicine".<sup>4-6</sup> Though AMR is a complex global challenge, key remedies are clear. Because of the huge cost in developing new antibiotics, new drugs are largely insufficient as our weapon to fight against AMR. In this case, the more effective way to suppress the development of AMR is to use narrow-spectrum antibiotics based on accurate diagnosis, preferentially, using antimicrobial susceptibility test (AST).<sup>7-9</sup> This requires AST techniques to be quick in returning results, convenient and cost-efficient to use, so as to save valuable time and resources in treatment of infections.

However, current AST methods are far from meeting these

requirements. An AST involves a large number of tests, especially when the minimum inhibitory concentration (MIC)<sup>10-11</sup> of each drug is desired. Although there are a variety of methods available for AST, like disc diffusion<sup>7-9</sup> and broth dilution test,<sup>12-13</sup> these methods are based on observing colony formation,<sup>14</sup> which is costly and time-consuming.<sup>15</sup> A similar challenge exists in the drug development which requires large-scale screening.<sup>16-17</sup> Tremendous efforts have been made to improve AST technology; however, those new strategies, based on PCR, nanoparticles, or dielectrophoresis, are still impractical to be used for real specimens, because of various types of interferences to the result.<sup>18-21</sup> New methods based on automated zone-readers are more reliable than standard disc diffusion techniques, yet these methods are still costly, require ancillary testing, and are limited by the growth rate of suspected bugs. Moreover, the accuracy of detecting the broad range of resistance phenotypes is still concerned (e.g., the Phoenix system showed a specificity of only 64.9%).<sup>20, 22</sup> Most recently, emerging techniques are developed based on microfluidic platforms.<sup>23-27</sup> These methods culture target cells in microfabricated channels or chambers with drug loaded, and use microscopy to detect the effect of drug<sup>28-30</sup>. These methods do not need the cells to grow into macroscopic colonies, and could therefore save time for analysis;<sup>31-36</sup> labour cost and operation error in pipetting are also significantly reduced. However, most of the on-chip methods are based on devices made of PDMS, which is easy to foul,<sup>37-39</sup> and the

<sup>a</sup> Department of Chemistry, Hong Kong Baptist University, Waterloo Rd, Kowloon, Hong Kong, China.

<sup>b</sup> State Key Laboratory of Environmental and Biological Analysis, The Hong Kong Baptist University, Waterloo Rd, Kowloon, Hong Kong, China

<sup>c</sup> HKBU Institute of Research and Continuing Education, Shenzhen, China

†Electronic Supplementary Information (ESI) available: [details of any supplementary information available should be included here]. See DOI: 10.1039/x0xx00000x

fouling effect is enhanced by the large surface-to-volume ratio of microchannels; it is revealed in various reports that the concentration of drugs inside a PDMS channel is hard to control precisely.<sup>40-43</sup> This becomes a fundamental problem of PDMS-based platform in quantitative applications, which are necessary for MIC tests. In all, users of current AST methods may suspect that in-channel incubation of bacteria would produce different results compared with traditional methods, thus be reluctant to accept microfluidic AST technologies.

Herein we propose a new strategy of AST which combines conventional plate culture with microfluidic technology. This strategy cultures cells on top of a microfluidic device made of hydrogel (rather than inside a microchannel); it eliminates the effect of shear flow and allows users to operate and interpret the result using their experience on conventional plate culture, while incorporating the advantages of microfluidics without the problem of channel fouling. To realize this idea, we developed a novel microfabrication method to produce inexpensive hydrogel microfluidic devices. Hydrogels are inherently biocompatible, and have long been the material for solid media cell culture; their porosity allows small molecules to penetrate and form gradient across concentration difference.<sup>44-49</sup> A mixture of agar and sodium alginate was used in this work. Agar solidifies under room temperature and makes it possible to cast the mixture gel; alginate crosslinks upon addition of  $\text{Ca}^{2+}$ , making it possible to bond the chip. The device we prepared was entirely made of hydrogel without any other structures as support or frame. Parallel channels were designed to generate a continuous and linear gradient. Bacterial samples were applied directly on top of the gel device, and incubated in the same manner as in traditional plate culture; as compared to cell culture inside microchannel, this setup is likely to generate culture results closer to those from the methods people have long been relying on. Also, two-dimensional tests were realized with almost the same ease with one-dimensional test, making it convenient to measure the synergistic effect of drugs and other environmental factors such as pH and oxidative substances from immune system, a task hard for traditional AST methods to accomplish. Though made of biodegradable materials, the device could last for appropriate period of time under proper storage conditions (no failure was detected after three months).

## Experimental

### 1. Materials and equipment

Agar, sodium alginate, Lysogeny broth (LB) powder (Lennox), fluorescein powder and other chemicals were purchased from Sigma-Aldrich. PDMS prepolymer (RTV 615) was obtained from Momentive Performance Materials (Waterford, NY). Heating plate was purchased from Xinruiqi Electronic, Inc. (LKTC-B1-T, China). The syringe pump was purchased from Cole-Parmer, US. The fluorescence microscopy used in the experiment was

obtained from Micro-shot Technology Limited (ML-30, China) equipped with Infinity 2 digital camera (Lumenera Corporation, Canada) to capture pictures. Miicraft®3D printer was obtained from Ankitst Exim Inc, India. Green fluorescence protein (GFP)-expressing *E. coli* was obtained from Hongkai Wu from Hong Kong University of Science and Technology.

### 2. Fabrication of agar-alginate mixed gel device

The initial templates were designed using AutoCAD 2015 and printed by 3D printer, from which the PDMS (10:1 ratio) reverse-mold was created. Molds and glass slides used in the following steps were sterilized with 75% ethanol. For every 10 mL of mixed gel, 0.15 g of agar, 0.15 g of sodium alginate and 0.2 g of LB broth powder were weighed, and deionized water was added to adjust the total volume to 10 mL, and the mixture was heated to boil and stirred until dissolved completely. Liquid gel was applied to PDMS molds and allowed to solidify, after which the solid gel pieces were moved onto glass slides and stacked to prepare for the bonding process.  $\text{CaCl}_2$  solution (0.5 M) was applied onto the surface of the gel device and spread evenly. The device was then heated at 55 °C and once the surface was dried,  $\text{CaCl}_2$  solution was applied again. The process was repeated twice on each side of the device until binding was complete, after which it was washed with autoclaved LB broth solution and exposed to UV-B (254 nm) treatment. In this work, different concentrations (1, 1.5 and 2 % (w/v)) of agar and (1, 1.5 and 2 % (w/v)) alginate were tested.

### 3. Investigation of the on-chip diffusion process

For one-dimensional test, fluorescein solution (100  $\mu\text{g}/\text{mL}$ ) and

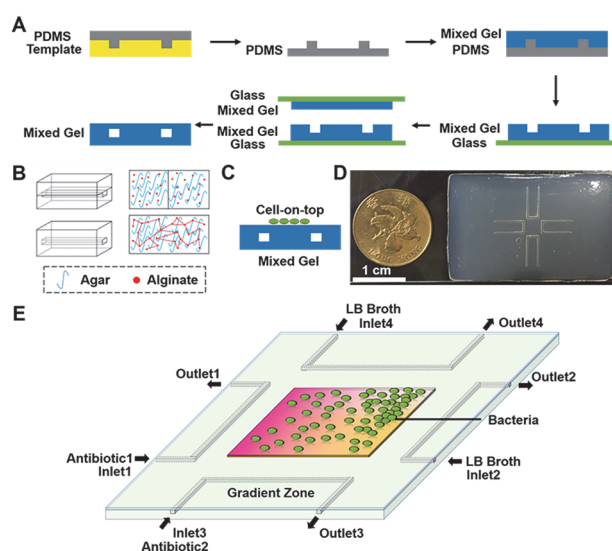


**Fig. 1** Schematics of the fabrication process of agar-alginate mixed gel device. (A) The fabrication process of the PDMS mold and the mixed gel. (B) The bonding mechanism of the mixed gel pieces. Upon addition of  $\text{Ca}^{2+}$  ions, alginate is crosslinked and bonds the mixed gel slides together. (C) Cells are cultured on top of the device. (D) Photo of a fabricated mixed-gel device. (E) Schematics of two-dimensional AST.

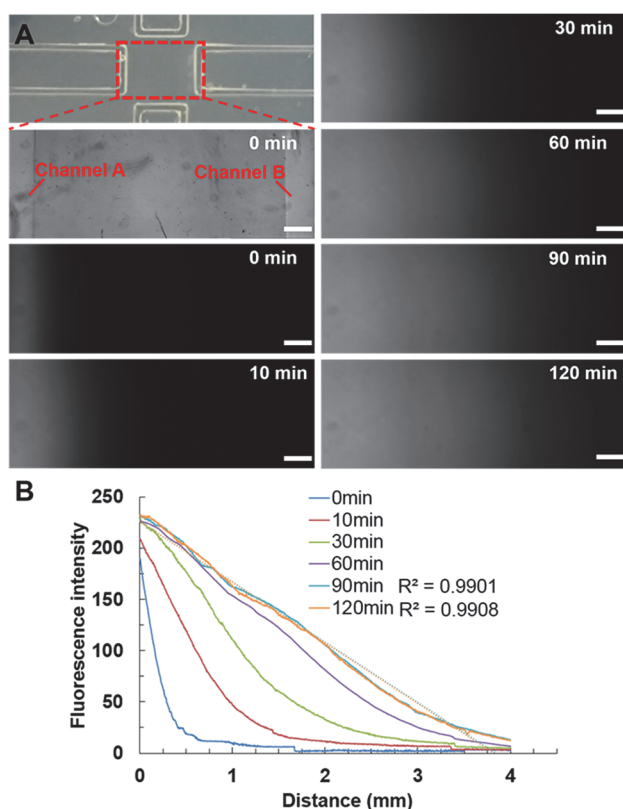


**Fig. 2** Diffusion test on the device. (A) The gradual process of diffusion-based gradient generation between the two channels. The front of fluorescein propagated to the right over time. (B) The fluorescein intensity versus the distance from the channel supplying fluorescein at multiple time points. The gradient stabilized at around 90 minutes, and achieved good linearity. The scale bars represent 300  $\mu\text{m}$ .

D.I. water were injected into the channels with a flow rate of 0.25 mL/h (Fig. 2 and Fig. S2). Images were taken by the fluorescence microscope and analyzed by ImageJ 1.4 software. For two-dimensional diffusion test, fluorescein (100  $\mu\text{g}/\text{mL}$ ) and rhodamine B (100  $\mu\text{g}/\text{mL}$ ) solutions were injected into two neighboring channels; D.I. water was injected into other two channels; flow rate was maintained at 0.25 mL/h (Fig. S3). Images were taken by fluorescence microscope and analyzed by ImageJ 1.4 software.

#### 4. Antibiotic sensitivity testing

For one dimensional AST, antibiotic solution (diluted to proper concentration in 2% (w/v) LB broth) and LB broth were injected into the channels, respectively, at flow rates same as described in diffusion test. Bacterial sample was diluted to appropriate density ( $\text{OD}_{600}=0.1$ ), one droplet (2-3  $\mu\text{L}$ ) of which was applied to the center of the device surface in between the channels. A sterilized Petri dish cap was used to cover the device and isolate it from the surroundings. The device was then incubated at 37  $^{\circ}\text{C}$  and images captured by fluorescence microscope and analyzed by ImageJ 1.4 software. For two-dimensional AST, antibiotic solutions that had been diluted to proper concentrations were injected into two neighboring

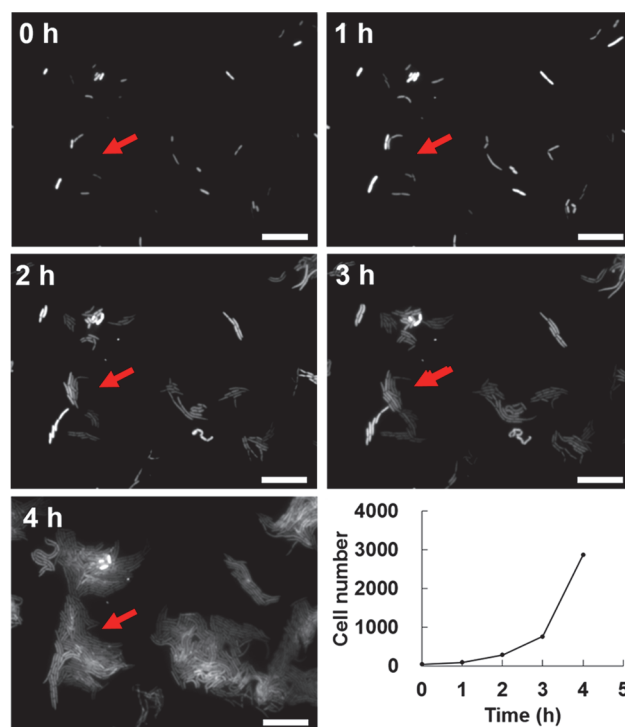


**Fig. 3** GFP-*E. coli* growth process with time. Fluorescence images (0h to 4 h) were recorded every 60 min at the same position. Gradual change from individual cells to larger colonies was observed for the bacterium cells near the arrow. The plot shows the number of cells in the area at each time point. The scale bars represent 10  $\mu\text{m}$ .

channels; LB broth was injected into the other two. Other procedures and conditions were the same as mentioned in one-dimensional AST experiment.

## Results and Discussion

### 1. Fabrication process of whole hydrogel microdevice

In our work the device was fabricated entirely in hydrogels, one of which is agar, an inexpensive gel widely-used as standard material in the culture of microorganisms. Agar is a natural product that has been used as gelling agent for over three centuries; it is actually a mixture of linear polysaccharide agarose and some smaller molecules called agaropectin. It is interesting to note that although this inexpensive material has been broadly used in cell culture, it was barely used in microfluidics; on the other hand, agarose, a purified component from agar was used for fabricating microfluidic chips, probably because of its better gelation performance/mechanical property. But agarose is about 20-fold the price of agar; and agar is the standard material for plate cell culture, which is extensively used and well trusted in cell biology. Hence, although agar is harder to microfabricate than agarose, we made special effort in this work to develop an effective method for fabricating microfluidic device using agar. In our experiment, this challenge was addressed by using a mixture of agar and alginate (1.5% (w/v) each), and unique

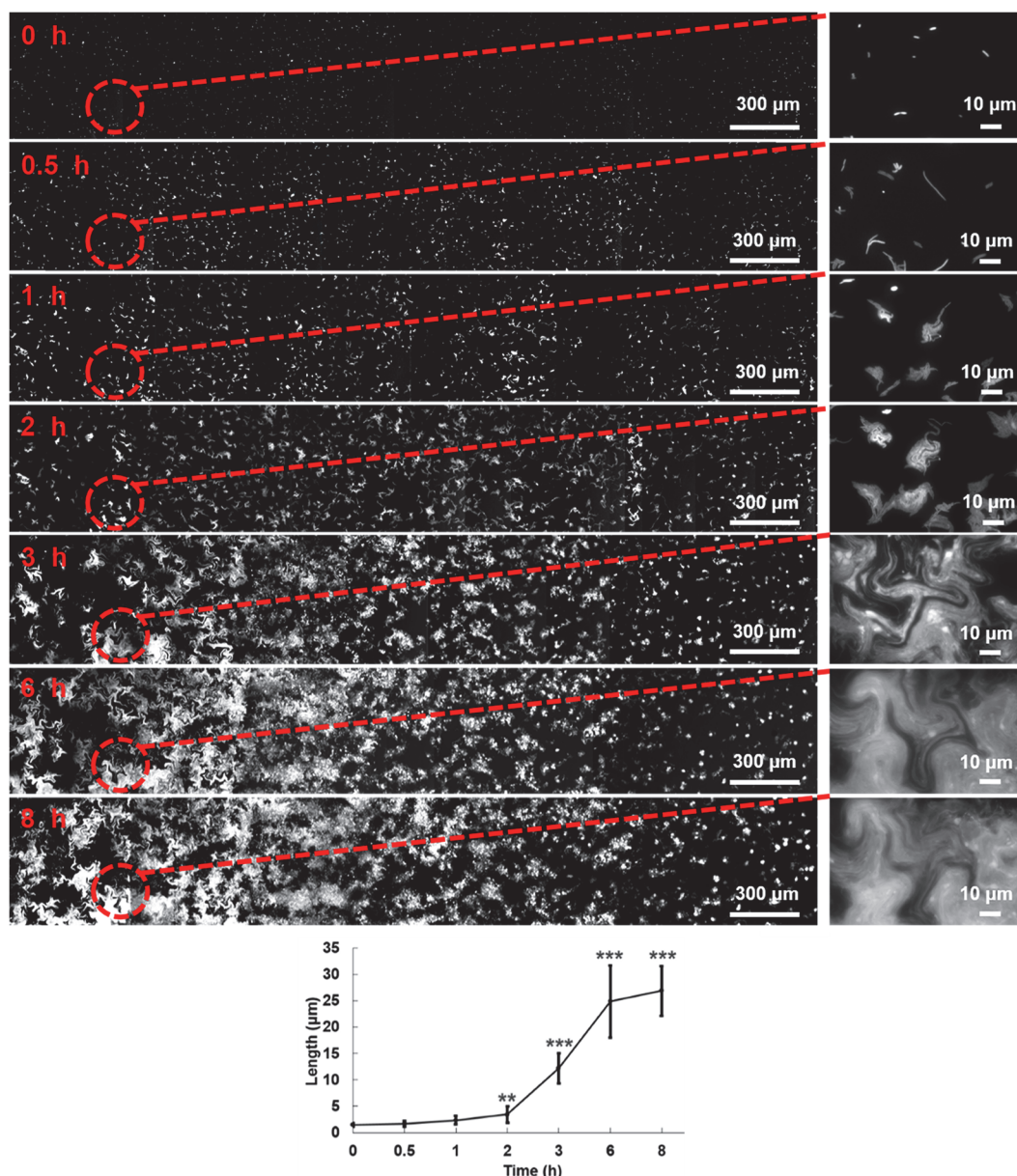


**Fig. 4** Antibiotic sensitivity testing of ampicillin (\*\*,  $P < 0.01$ ; \*\*\*,  $P < 0.001$ ). *E. coli* cells were treated with ampicillin for 8 hours. The circles indicate the area under MIC value. The plot shows the average length of bacterium cells inside the circled area.

method for casting the structures and bonding the chip. The minimum dimension of the structure was  $100 \mu\text{m}$  and the thinnest thickness of the gel which can be peeled off from the PDMS mold was about  $500 \mu\text{m}$  (Fig. S1A). As shown in Fig. 1, two pieces of gel slides were cast and then bonded using  $\text{CaCl}_2$  solution. Before adding  $\text{Ca}^{2+}$ , the mixture of agar and alginate was tender, making the conformal sealing of channel difficult. To obtain high yield of bonding, we designed a “dried” diffusion bonding method. After the two gel slides were adhered together, high concentration  $\text{Ca}^{2+}$  solution ( $0.5 \text{ M}$ ) was applied onto the surface of the gel device in droplets and spread evenly. The device was then heated at  $55 \text{ }^\circ\text{C}$  and once the surface was dried,  $\text{CaCl}_2$  solution was applied again. Applying the solution only once was determined as inadequate, resulting incomplete bonding between the two layers such that the device was easy to be damaged during operation,

while repeated application for more than twice didn’t improve upon the already good bonding performance of the gel layers. Thus we decided to apply  $\text{Ca}^{2+}$  solution twice on each side of the device. This process would deliver enough  $\text{Ca}^{2+}$  ions to the bonding interface while limiting the amount of water soaked in the gel; otherwise the channels are easy to deform and be blocked after bonding. The device was washed with LB broth after  $\text{CaCl}_2$  treatment, to eliminate free  $\text{Ca}^{2+}$  ions and avoid their adverse effect to bacterial growth. The concentration of  $1.5\%$  agar and  $1.5\%$  alginate respectively was chosen as the finalized formula, because it offered a balance between flexibility and strength, as well as acceptable optical transparency. In 15 minutes, the liquid gel would cool down and solidify, allowing peeling of gel pieces from molds. We found that treatment to make the inner surface of the PDMS mold more hydrophobic could assist the removal, and reduce

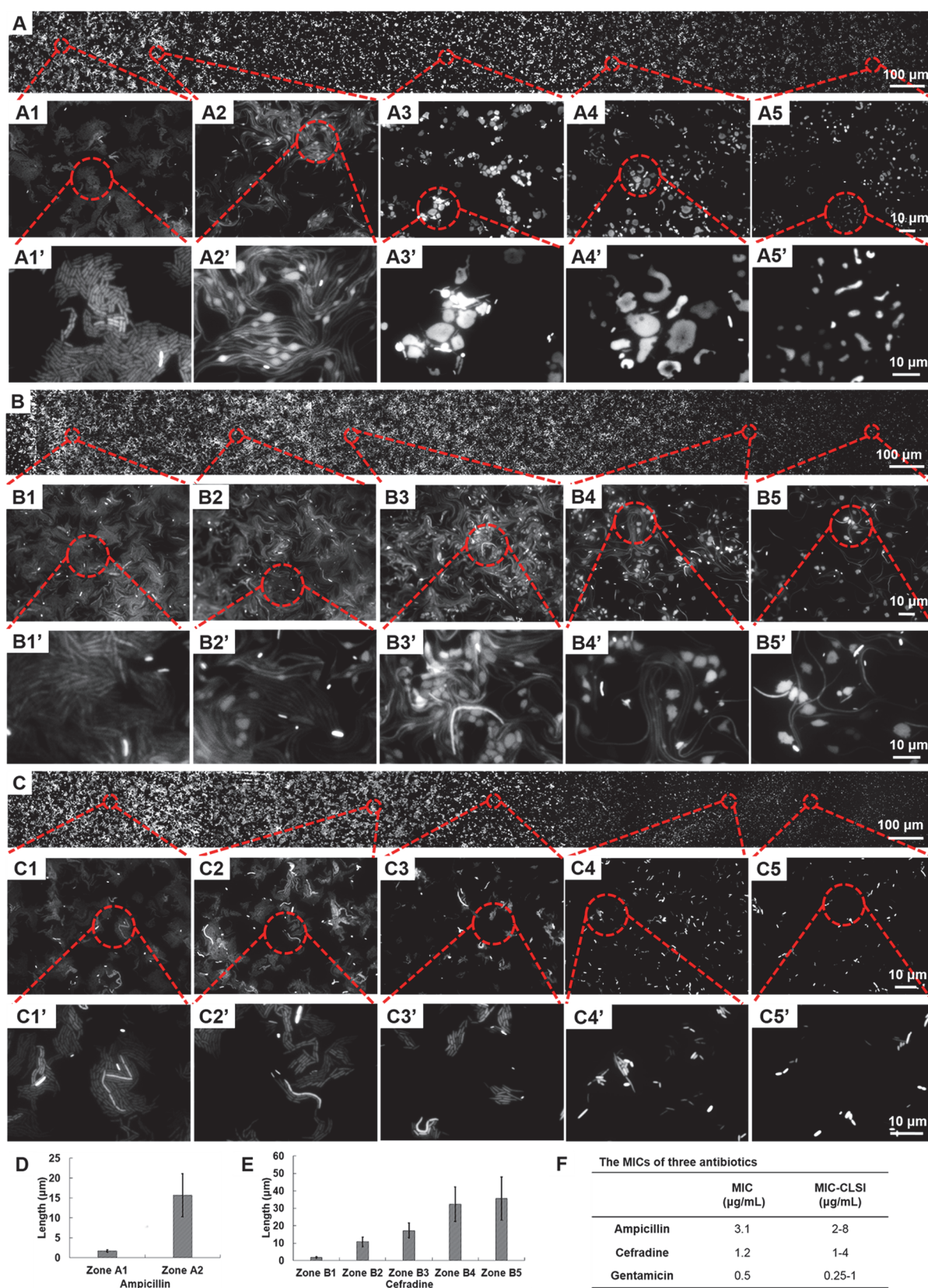


**Fig. 5** Antibiotic susceptibility testing of GFP *E. coli* using different antibiotics ((A) ampicillin, (B) cefradine and (C) gentamicin). In each fluorescence image, a gradual change from normal bacterial growth to inhibited growth could be observed from left to right. The zoom-ins show the change of cell morphology at different drug concentrations. The bar charts (D-E) show the average length of *E. coli* cells in each zone examined in ampicillin and cefradine trials; Zone A2, B2 were chosen as the critical point of inhibition. (F) The table gives the MIC values calculated from image analysis, comparing with standards from CLSI.<sup>54</sup>

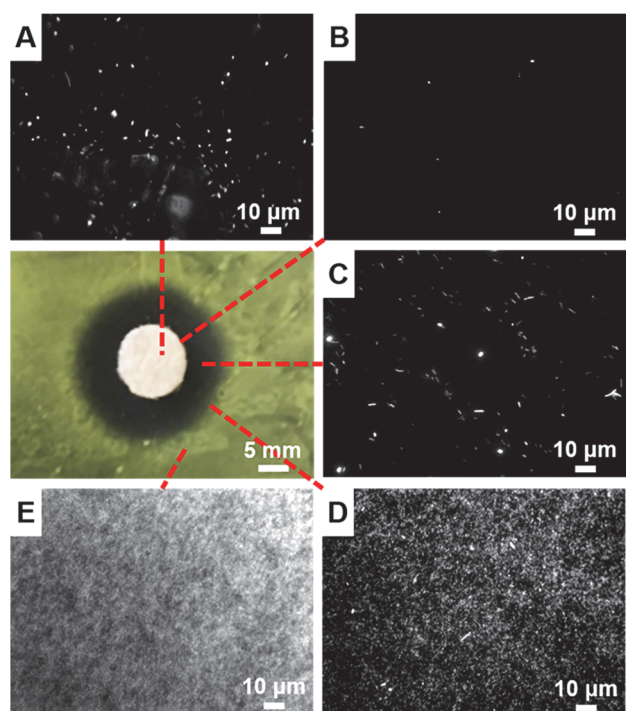


**Fig. 6** Microscopic inspection of agar disk diffusion test. (A: on the drug-loaded paper; B: paper edge; C: inside of inhibition zone; D: edge of inhibition zone; E: out of inhibition zone).

the chance of generating defects. We also studied the maximum flow rate of the channels to evaluate the bonding performance. The device was damaged at linear flow rate much higher than the flow rate normally needed (Fig. S1B). Also, the device could also be stored at 4 °C while submerged in Ca<sup>2+</sup>/LB solution for a prolonged period of time (no failure was detected after three months). The entire system for analysis consists of a microscope, microflow pumps and a heating plate. The microscope and the heating plate are equipment commonly found in clinical and research laboratories, while the need for microflow pumps could be eliminated by gravity-driven flows used in microfluidic devices.<sup>50</sup>

## 2. Diffusion test of the whole hydrogel device

A diffusion test was carried out using two parallel channels (300 μm) which were 4 mm apart on the device. As the pore sizes of agar and alginate are both larger than typical antibiotic molecules,<sup>51-52</sup> the diffusion behaviour of antibiotics in our gel device would be close to that in free solution. The diffusion of molecules in free solution could be described using equations expressing the diffusion coefficient and in these equations the only factor related to the diffusing solute is the size of the suspended molecules.<sup>53</sup> In this case, fluorescein (M.W. 332 g/mol) was used as sample as it has a molecular weight similar to that of many commonly used antibiotics, thus it would behave in a similar manner when diffusing across the hydrogel mixture.<sup>25</sup> The fluorescein molecules diffused from channel A to B and excess fluorescein was taken away by D.I. water in channel B. As a result, a stable gradient with good linearity was

formed between the two channels. Note that different from many gel diffusive methods such as disk diffusion for AST, our method can generate a precisely controlled gradient over a long period of time, because both the source and the drain of the gradient are continuously refreshed by the flow inside microchannels. Fig. 2 shows the diffusion-based gradient stabilized at around 90 minutes, and there was limited difference between results at 90 and 120 minutes. Also, as Fig. S2 suggests, the gradient was also spread evenly over the direction perpendicular to its propagation.

## 3. AST on the whole hydrogel device

The results in diffusion tests indicated that our devices achieved good linearity and stability in diffusion-based gradient generation. We performed AST experiments to further evaluate the performance of the system. 2% (w/v) LB broth was used to dilute of antibiotic solutions in this work, resulting in the same concentration of the LB broth used in the parallel channel and the hydrogel device itself. Consequently, the concentration of LB broth became even and stable across the whole device and it would not cause the differences in the bacterial growth. Green fluorescence protein (GFP)-expressing *E. coli* cells were employed as bacterial samples. Firstly, normal bacterial growth test was performed on our device. As shown in Fig. 3, the *E. coli* cells grew into large colonies over time; a roughly two-fold increment every 30 minutes was observed, which is consistent with normal agar plate culture of *E. coli*. Then, we tested three antibiotics, ampicillin (M.W. 349 g/mol), cefradine (M.W. 349 g/mol), and gentamicin (M.W. 477 g/mol). The tested drugs have molecular weights close to that of fluorescein used for diffusion test, and were expected to diffuse in a similar manner, generating predictable linear gradients. The concentration ranges of drugs were set according to Clinical and Laboratory Standards Institute (CLSI) data.<sup>54</sup> Fig. 4 depicts the AST result of ampicillin, one of the β-lactam class antibiotics that function by inhibiting the bacterium cell wall synthesis, resulting in weak cell structure and ultimately the lysis of bacteria. The inhibition of normal bacterial growth was continuously tracked within 8 hours and the lengths of cells at different locations were measured. As ampicillin takes its effect on the bacteria, the latter grow abnormally in length, which is used as indication of inhibition, because these bacteria eventually die.<sup>55</sup> Therefore, the MIC values could be determined in this area by calculating the concentration of antibiotics. At higher concentration (on the right side of the image), cells swelled and eventually burst. The plotting suggests that elongation of cells was significant enough at around 2 to 3 hours by when MIC values could be calculated. Hence, the MIC values of these antibiotics were calculated after 3 hours of test (Fig. 5). To calculate the MIC value, the inhibition point was located with image analysis tools, and the precise deterministic rules were depending on the kind of bacteria.<sup>56</sup> For ampicillin, the point was identified as A2 in Fig. 5. Using the location of this point between the two channels, the corresponding drug concentration at this point was calculated from the linear gradient plot obtained in the diffusion test, showing the reduction from 100% drug

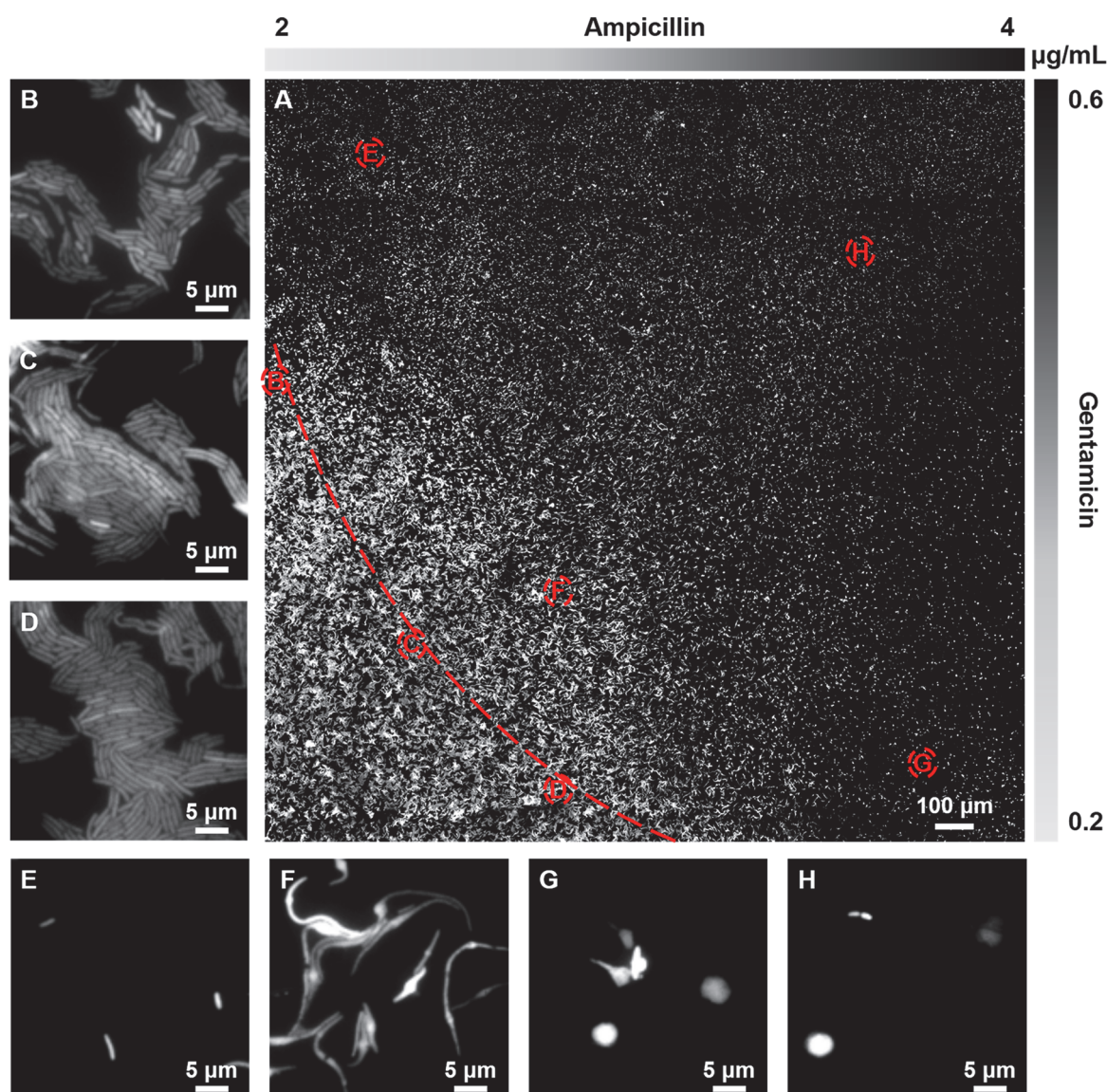


**Fig. 7** Two-dimensional AST for combined drug study using GFP *E. coli* as sample. (A) Ampicillin gradient ran from the right to the left, while gentamicin gradient was generated from the top to the bottom on the device. The red dotted line presents an inhibition boundary of two drugs. (B-H) The morphologies of *E. coli* at different concentrations of two antibiotics.

concentration to blank. The MIC value for ampicillin was calculated to be 3.1  $\mu\text{g/mL}$ . Like ampicillin, cefradine is also one of the  $\beta$ -lactam antibiotics, and acts in similar manner. This similarity in working mechanism was shown in the results. Affected *E. coli* also displayed elongation and swelling, but of less extent compared with ampicillin, and there was no obvious cell bursting observed. The MIC value of cefradine was 1.2  $\mu\text{g/mL}$ . Being one of the aminoglycosides antibiotics, gentamicin is in a different class from the above mentioned two drugs. It functions by binding irreversibly to bacterial ribosome and interrupting protein synthesis. As a result, bacteria were observed to cease their growth all together, with no obvious morphological changes. Thus, the MIC value of gentamicin was determined by counting cell numbers in a given area and the result was 0.5  $\mu\text{g/mL}$ . All the MIC values of these antibiotics were in accordance with the data from CLSI.

Compared to traditional methods, our device could obtain the MIC value within 3 hours, which significantly accelerates the diagnosis. A control experiment based on traditional disk diffusion method was performed. Fig. 6 shows the results of AST of GFP *E. coli* using gentamicin, which took much longer time and could not support single-cell level monitoring at different drug concentrations due to the changing gradient. Also, comparing to those ASTs based on microfluidic methods, on-chip-top culture provided the bacteria with growth conditions more similar to traditional methods, e.g., on hydrogel surface and without shear flow.<sup>57</sup> Moreover, the cells at any position could be conveniently collected at any time for other tests, which is difficult to realize by cell-in-channel microfluidic methods. Moreover, the system is expected to be more convenient for current AST users to upgrade to. Finally, these devices are made entirely from cheap and biodegradable

materials, and are compatible with current disposal protocols in clinical labs.

Another significant advantage of the cell-on-hydrogel device is that two-dimensional AST could be carried out conveniently. Rhodamine B and fluorescein were chosen for a two-dimensional diffusion test. The results (Fig. S3) indicate that the two types of dye molecules diffused along their directions and no obvious interference was detected, and two gradients with good linearity were obtained and shown in the photos. The formation of the two perpendicular gradients serves as the basis for the experiments of two-dimensional AST involving two different antibiotics. The intersecting area to inspect was a square that has a width of 2 mm and grids were fabricated in the hydrogel to help conveniently locate the inspection area (Fig. S4). Ampicillin and gentamicin, which have cooperative effect in clinical applications, were chosen as the tested drugs. As shown in Fig. 7, ampicillin gradient ran from right to left of the image while gentamicin gradient spread from top to bottom. The two drugs created a combined inhibition effect starting from the top left corner to the bottom right, decreasing in strength. The resulted inhibition boundary was observed to be roughly perpendicular to this diagonal line. Though our device performed well when using GFP *E. coli* and fluorescence microscope, a further question was how this novel technique would handle real samples in practical uses. Normal bacterium cells do not produce fluorescence proteins, and thus make the inspection more difficult. However, it was found that the transparency of the device allowed inspection of wild-type bacteria without the use of fluorescence mode, demonstrating the potential of examining real samples (Fig. S5-S6). As a result, we successfully obtained the MIC values of *E. coli* (ATCC 25922) and *S. aureus* (ATCC 29213), and both were in accordance with the data from CLSI.

## Conclusions

In conclusion, we demonstrated an innovative and convenient method to perform cell-on-hydrogel AST. The device was made of an inexpensive formula consisting of two kinds of hydrogels, agar for culturing cells and alginate for sealing the channels. A stable linear gradient of antibiotic was generated in the device by molecule diffusion. Meanwhile, the cellular morphology under different drug concentrations and the MIC value of antibiotic were conveniently obtained within 2-3 hours. Our strategy allows seamless connection to conventional AST, while incorporating the advantages of microfluidics; meanwhile, the cell-on-chip design eliminates the potential problem of shear flow, and the hydrogel chip avoids the channel fouling issue. The convenience of conducting two-dimensional AST allows our system to be employed in investigation of the synergistic effect of drugs as well as other factors such as pH and oxidative substances from the immune system. Moreover, our device could be simplified by the use of pumpless design, in which the mechanical pumps are replaced by gravity-driven systems similar to infusion. This should further reduce the equipment needed and enable broader applications of this device. Finally, the technique for

fabricating inexpensive hydrogel chip could be useful for other applications as well.

## Acknowledgements

The authors thank Prof. Hongkai Wu from Hong Kong University of Science and Technology for constructive discussion on the fabrication of hydrogel microfluidic chips. This work was supported by the Hong Kong RGC (#22200515), NSFC (21505110), and Hong Kong Baptist University (FRG2/14-15/072, SDF 03-17-096).

## References

- 1 Antimicrobial resistance, *WHO Fact sheet* N°194, 2014.
- 2 "Antibiotic Resistance Questions & Answers". Get Smart: Know When Antibiotics Work. Centers for Disease Control and Prevention, USA. 2009.
- 3 H. C. Davison, J. C. Low and M. E. Woolhouse, *Trends Microbiol*, 2000, **8**, 554
- 4 Antimicrobial resistance: global report on surveillance, *WHO*, 2014.
- 5 A. Kamradt-Scott, *PLoS Med.*, 2011, **8**: e1001021.
- 6 D. Wernli, T. Haustein, J. Conly, Y. Carmeli, I. Kickbusch and S. Harbarth, *PLoS Med.*, 2011, **8**: e1001022.
- 7 J. H. Jorgensen and M. J. Ferraro, *Clin. Infect. Dis.*, 2000, **30**, 799.
- 8 D. Felmingham and D. F. J. Brown, *J. Antimicrob. Chemother.*, 2001, **48**, 81.
- 9 J. H. Jorgensen and M. J. Ferraro, *Clin. Infect. Dis.*, 2009, **49**, 1749.
- 10 J. M. Andrews, *J. Antimicrob. Chemother.*, 2001, **48**, 5.
- 11 J.D. Turnidge, M.J. Ferraro and J.H. Jorgensen, *Manual of Clinical Microbiology*, 8th Ed, *American Society of Clinical Microbiology*, 2003, 1103.
- 12 M. R. Pulido, M. Garcia-Quintanilla, R. Martin-Pena, J. M. Cisneros and M. J. McConnell, *J. Antimicrob. Chemother.*, 2013, **68**, 2710.
- 13 M. Fredborg, K. R. Andersen, E. Jørgensen, A. Droce, T. Olesen, B. B. Jensen, F. S. Rosenvinge and T. E. Sondergaard, *J. Clin. Microbiol*, 2013, **51**, 2047.
- 14 G. V. Doern, *J. Clin. Microbiol*, 2011, **49**, S4.
- 15 H. Dickert, K. Machka and I. Braveny, *Infection*, 1981, **9**, 18.
- 16 A. Dalhoff, P.G. Ambrose and J.W. Mouton, *Infection*, 2009, **37**, 296.
- 17 M. Lehtopolku, P. Kotilainen, P. Puukk, U. M. Nakari, A. Siitonen, E. Eerol, P. Huovinen and A. J. Hakanena, *J. Clin. Microbiol*, 2012, **50**, 52.
- 18 J.M. Rolain, M.N. Mallet, P.E. Fournier and D. Raoult, *J. Antimicrob. Chemother.*, 2004, **54**, 538.
- 19 J. C. Cheng, C. L. Huang, C. C. Lin, C. C. Chen, Y. C. Chang, S. S. Chang and C. P. Tseng, *Clin. Chem.*, 2006, **52**, 1997.
- 20 C. Kaittani, S. Santra and J. M. Perez, *Adv. Drug Deliv. Rev.*, 2010, **62**, 408.
- 21 S. Nath, C. Kaittani, A. Tinkham and J. M. Perez, *Anal. Chem.*, 2008, **80**, 1033.
- 22 K. C. Carroll, A. P. Borek, C. Burger, B. Glanz, H. Bhally, S. Henciak and D. C. Flayhart, *J. Clin. Microbiol.*, 2006, **44**, 2072-2077.
- 23 A. D. Stroock, S. K. W. Dertinger, A. Ajdari, I. Mezić, H. A. Stone



- and G. M. Whitesides, *Science*, 2002, **295**, 647-651.
- 24 K.N. Ren, J.H. Zhou and H. K. Wu, *Acc. Chem. Res.*, 2013, **46**, 2396-2406.
- 25 J. Choi, Y. G. Jung, J. Kim, S. Kim, Y. Jung, H. Na and S. Kwon, *Lab Chip*, 2013, **13**, 280-287.
- 26 C. H. Chen, Y. Lu, M. L. Y. Sin, K. E. Mach, D. D. Zhang, V. Gau, J. C. Liao and P. K. Wong, *Anal. Chem.*, 2010, **82**, 1012.
- 27 R. Mohan, A. Mukherjee, S. E. Sevgen, C. Sanpitakseree, J. Lee, C. M. Schroeder and P. J. A. Kenis, *Biosens. Bioelectron.*, 2013, **49**, 118.
- 28 M. Kalashnikov, J. C. Lee, J. Campbell, A. Sharon and A. F. Sauer-Budge, *Lab Chip*, 2012, **12**, 4523-4532.
- 29 I. Peitz and R. V. Leeuwen, *Lab Chip*, 2010, **10**, 2944-2951.
- 30 J. Choi, J. Yoo, K. J. Kim, E. G. Kim, K. O. Park, H. Kim, H. Kim, H. Jung, T. Kim, M. Choi, H. C. Kim, S. Ryoo, Y. G. Jung and S. Kwon, *Appl. Microbiol. Biot.*, 2016, **1**, 11.
- 31 K.N. Ren, Y. Chen and H. K. Wu, *Curr. Opin. Biotechnol.*, 2014, **25**, 78-85.
- 32 X. Mu, W. F. Zheng, J. S. Sun, W. Zhang and X. Y. Jiang, *Small*, 2013, **9**, 9-21.
- 33 C.H. Chen, Y. Lu, M. L. Y. Sin, K. E. Mach, D. D. Zhang, V. Gau, J. C. Liao and P. K. Wong, *Anal. Chem.*, 2010, **82**, 1012-1019.
- 34 B. Xiong, K.N. Ren, Y.W. Shu, Y. Chen, B. Shen and H. K. Wu, *Adv. Mater.*, 2014, **26**, 5525-5532.
- 35 R. L. Frisch and S. M. Rosenberg, *Science*, 2011, **333**, 1713.
- 36 Q. Zhang, G. Lambert, D. Liao, H. Kim, K. Robin, C. Tung, N. Pourmand and R. H. Austin, *Science*, 2011, **333**, 1764.
- 37 R. Mukhopadhyay, *Anal. Chem.*, 2007, **79**, 3248.
- 38 J. N. Lee, C. Park and G. M. Whitesides, *Anal. Chem.*, 2003, **75**, 6544.
- 39 J. L. Pittman, C. S. Henry and S. D. Gilman, *Anal. Chem.*, 2003, **75**, 361.
- 40 K.N. Ren, Y.H. Zhao, J. Su, D. Ryan and H.K. Wu, *Anal. Chem.*, 2010, **82**, 5965-5971.
- 41 M. W. Toepke and D. J. Beebe, *Lab Chip*, 2006, **6**, 1484.
- 42 L. Gui and C. L. Ren, *Appl. Phys. Lett.*, 2008, **92**, 024102.
- 43 K.N. Ren, W. Dai, J. H. Zhou, J. Su and H. K. Wu, *Proc. Natl. Acad. Sci.*, 2011, **108**, 8162-8166.
- 44 N. A. Peppas, J. Z. Hilt, A. Khademhosseini and R. Langer, *Adv. Mater.*, 2006, **18**, 1345-1360.
- 45 S. Y. Cheng, S. Heilman, M. Wasserman, S. Archer, M. L. Shuler and M. M. Wu, *Lab Chip*, 2007, **7**, 763-769.
- 46 X. T. Shi, J. H. Zhou, Y. H. Zhao, L. Li and H. K. Wu, *Adv. Healthcare Mater.*, 2013, **2**, 846-853.
- 47 X. Mu, W. F. Zheng, L. Xiao, W. Zhang and X. Y. Jiang, *Lab Chip*, 2013, **13**, 1612-1618.
- 48 T. M. Keenan and A. Folch, *Lab Chip*, 2008, **8**, 34-57.
- 49 J. Atencia, G. A. Cooksey and L. E. Locascio, *Lab Chip*, 2012, **12**, 309-316.
- 50 M. Marimuthu and S. Kim S, *Anal. Biochem.*, 2013, **437**, 161-163.
- 51 G. K. Ackers and R. L. Steere, *Biochim. Biophys. Acta.*, 1962, **59**, 137-149.
- 52 T. Boonthekul, H. J. Kong and D. J. Mooney, *Biomaterials*, 2005, **26**, 2455-2465.
- 53 A. Einstein, *Investigations on the Theory of the Brownian Movement*, Courier Corporation, 1956.
- 54 Clinical and Laboratory Standards Institute (CLSI). Performance standards for antimicrobial susceptibility testing: 23rd informational supplement (M100-S23). Wayne, PA: CLSI; 2013
- 55 T. Sandberg, K. Stenqvist and C. Svanborg-Edén, *Review of Infectious Diseases*, 1979, **1**, 838-844.
- 56 J. Choi, J. Yoo, M. Lee, E. G. Kim, J. S. Lee, S. Lee, S. Joo, S. H. Song, E. C. Kim, J. C. Lee, H. C. Kim, Y. G. Jung and S. Kwon, *Sci. Transl. Med.*, 2014, **6**, 267ra174-267ra174.
- 57 J.H. Zhou, K.N. Ren, W. Dai, Y.H. Zhao, D. Ryan and H.K. Wu, *Lab Chip*, 2011, **11**, 2288-2294.